

# The Role of PLIN3 in Prognosis and Tumor-Associated Macrophage Infiltration: A Pan-Cancer Analysis

Shaohua Yang<sup>1-3,\*</sup>, Hejie Liu<sup>4,\*</sup>, Youbin Zheng<sup>5,\*</sup>, Hongyu Chu<sup>6</sup>, Zhuming Lu<sup>4</sup>, Jie Yuan<sup>1,2</sup>, Shengshan Xu<sup>4</sup>

<sup>1</sup>Department of General Surgery, Foshan Clinical Medical School, Guangzhou University of Chinese Medicine, Foshan, Guangdong, People's Republic of China; <sup>2</sup>Department of General Surgery, Foshan Fosun Chancheng Hospital, Foshan, Guangdong, People's Republic of China; <sup>3</sup>Institute of Gastroenterology, the First Affiliated Hospital of Guangzhou University of Chinese Medicine, Guangzhou, Guangdong, People's Republic of China; <sup>4</sup>Department of Thoracic Surgery, Jiangmen Central Hospital, Jiangmen, Guangdong, People's Republic of China; <sup>5</sup>Department of Radiology, Jiangmen Wuyi Hospital of Traditional Chinese Medicine, Jiangmen, Guangdong, People's Republic of China; <sup>6</sup>Department of Gastrointestinal, Colorectal and Anal Surgery, China-Japan Union Hospital of Jilin University, Changchun, Jilin, People's Republic of China

\*These authors contributed equally to this work

Correspondence: Jie Yuan; Shengshan Xu, Email yuanj1282024@163.com; xushengshan97@163.com

**Background:** Nucleolar and spindle-associated protein 1 (PLIN3), a member of the perilipin family, plays a critical role in lipid droplet dynamics and is implicated in promoting tumor progression across several cancers. However, its influence on the tumor immune microenvironment and its potential as a prognostic indicator regarding immunotherapy responses have yet to be systematically evaluated. This study leverages data retrieved from multiple databases to address these questions.

**Methods:** PLIN3 mRNA and protein expressions were analyzed across a diverse range of normal and cancerous tissues, utilizing data retrieved from multiple databases. The potential of PLIN3 as a diagnostic and prognostic biomarker in cancers was assessed. Advanced computational algorithms were employed to examine the impact of PLIN3 on immune cell infiltration. The association between PLIN3 expression and the presence of M2 macrophages was validated through analyses incorporating bulk and single-cell transcriptomics, spatial transcriptomics, and multicolor fluorescence staining techniques. Furthermore, the effects of PLIN3 on tumor malignancy and growth were investigated in vitro in lung adenocarcinoma (LUAD) cells. Potential compounds targeting PLIN3 were identified using the Connectivity Map (cMap) web tool, and their efficacy was further assessed through molecular docking.

**Results:** PLIN3 was predominantly upregulated in various cancers, correlating with adverse prognostic outcomes. A strong positive association was observed between PLIN3 levels and M2 macrophage infiltration in several cancer types, establishing it as a potential pan-cancer marker for M2 macrophage presence. This was confirmed by integrative multi-omics analysis and multiple fluorescence staining. Additionally, PLIN3 knockdown in LUAD cells diminished their malignant traits, resulting in decreased proliferation and migration. In LUAD, clofibrate was identified as a potential inhibitor of PLIN3's pro-oncogenic functions.

**Conclusion:** PLIN3 may serve as a potential biomarker and oncogene, particularly in LUAD. It plays a key role in mediating M2 macrophage infiltration in various cancers and presents a promising immunotherapeutic target.

**Keywords:** pan-cancer analysis, M2 macrophage, biomarker, prognosis, immunotherapy

## Introduction

Cancer remains a significant cause of mortality globally and poses a substantial public health challenge. Data from the Global Cancer Research Center indicated that in 2020, approximately 10 million cancer-related deaths occurred globally (excluding non-melanoma skin cancers). Projections suggest that by 2040, the global cancer burden could escalate to 28.4 million cases, marking a 47% increase from 2020.<sup>1</sup> Despite improvements in surgical techniques and early screening that have lowered mortality, tumor heterogeneity and their tendency to recur and metastasize contribute to poor prognosis and survival in multiple cancers.<sup>2</sup> Prognostic biomarkers and detailed patient characteristics are crucial for tailoring

treatments and enhancing patient outcomes.<sup>3,4</sup> Despite the increasing support for personalized cancer therapies, the integration of prognostic biomarkers into clinical practice remains limited.

Tumor-associated macrophages (TAMs), especially the M2 subtype, are pivotal in cancer development and progression. As central players in the tumor microenvironment, M2 macrophages drive tumor growth by stimulating angiogenesis, inhibiting anti-tumor immunity, and supporting metastatic spread.<sup>5</sup> Through the release of cytokines and growth factors, they establish an immunosuppressive niche that aids cancer cells in escaping immune detection.<sup>6</sup> Their presence is often linked to unfavorable outcomes in numerous malignancies, highlighting their potential as therapeutic targets.<sup>7</sup> Investigating the regulatory mechanisms behind M2 macrophage recruitment and activity is thus crucial for advancing cancer treatment strategies.

PLIN3, a member of the perilipin (PLIN) family, is integral to the synthesis and turnover of neutral lipids and is essential for cell viability and autophagy, potentially contributing to treatment resistance.<sup>8–10</sup> Previous research has demonstrated that PLIN3 is involved in macrophage transformation and enhances the expression of Toll-like receptor 9, thereby activating the immune response.<sup>11,12</sup> Studies have shown that PLIN3 can drive tumor progression in various cancers, including renal clear cell carcinoma, oral squamous cell carcinoma, liver cancer, cervical cancer, and prostate cancer.<sup>13–18</sup>

Pan-cancer analysis offers valuable insights into the roles and molecular underpinnings of specific genes in cancer, facilitating their potential clinical application.<sup>19</sup> Given the scarcity of comprehensive studies on PLIN3 across cancer types and its unexplored roles, this study undertook a broad pan-cancer analysis using publicly available databases to assess PLIN3's expression, genomic alterations, and prognostic significance. We also examined PLIN3's involvement in DNA damage response, cancer immunity, and epigenetic modifications. Furthermore, multiple fluorescence staining suggested that PLIN3 may serve as a marker for M2 macrophage infiltration across various cancers. The potential activation of PLIN3 by specific compounds in certain cancers was investigated, enhancing our understanding of PLIN3's functions across different tumors and suggesting new avenues for therapeutic interventions.

## Materials and Methods

### Collection and Analysis of Pan-Cancer Data

PLIN3-related clinical and gene expression data from various cancer and normal tissues were sourced from the TCGA and GTEx databases and processed using the UCSC Xena tool.<sup>20</sup> Gene expressions were standardized to transcripts per million (TPM). Subsequently, the standardized values were log-transformed using the formula  $\log_2(\text{TPM} + 1)$ . PLIN3 expression in tissues, visualized through immunohistochemistry (IHC) images, was accessed from the Human Protein Atlas (HPA).<sup>21</sup> Additionally, pan-cancer single-nucleotide variations (SNV) and merged methylation data from HM27 and HM450 platforms were retrieved from cBioPortal.<sup>22</sup> The abbreviations for the various cancers are provided in [Supplementary Table 1](#).

### PLIN3 Expression Evaluation Across Cancers

We analyzed PLIN3 expression in 33 cancer types using the TCGA dataset. To compare PLIN3 expression between cancerous and normal tissues, we utilized normal tissue data from the GTEx database, which includes samples from healthy individuals without cancer. Expression relationships with clinicopathological features such as cancer subtypes and TNM stages were illustrated using boxplots created with the “limma” and “ggplot2” R packages.<sup>23</sup> Comparative analysis of PLIN3 protein levels between cancerous and normal tissues employed data from the Clinical Proteomic Tumor Analysis Consortium (CPTAC), accessed via the UALCAN portal.<sup>24</sup> This dataset includes protein expression profiles from tumor samples and, where available, matched normal tissues from healthy individuals.

### Prognostic and Diagnostic Utility of PLIN3

The diagnostic utility of PLIN3 was assessed through ROC curves generated by the “pROC” package in R, with the diagnostic significance highlighted by the areas under the curves (AUCs). Prognostic assessments were conducted using univariate Cox regression for outcomes like overall survival (OS), disease-specific survival (DSS), disease-free survival (DFS), and progression-free survival (PFS), utilizing the “survival” and “forestplot” packages in R. Kaplan-Meier survival analysis is conducted using the “survival” R package. Optimal cutoff values for defining high and low expression cohorts are

established with the “survminer” R package, ensuring that neither group constitutes less than 30% of the sample. The differences between these expression groups were assessed using a Log rank test, executed via the “survfit” function.

## Analysis of Genomic Alterations and Genetic Heterogeneity in PLIN3

Genetic alterations of PLIN3 in pan-cancer were explored using the cBioPortal (<http://cbioportal.org>) and COSMIC (<https://cancer.sanger.ac.uk/cosmic/>) databases, focusing on mutation types and differences. The distribution of mutations within PLIN3 was illustrated using the “lollipopPlot” function from the “maftools” R package, with protein domains referenced from the PFAM database.

Tumor mutation burden (TMB) was calculated using the “maftools” R package. Microsatellite instability (MSI), homologous recombination deficiency (HRD), aneuploidy scores, and various mutation rates were assessed based on data extracted from existing literature.<sup>25</sup> Associations between these genomic features and PLIN3 expression levels were comprehensively evaluated.

## PLIN3’s Role in DNA Repair, Cancer Stemness, and Methylation

Interactions between PLIN3 expression and key DNA repair and methylation enzymes, including mismatch repair (MMR) genes<sup>26</sup> and DNA methyltransferases (DNMTs)<sup>27</sup> were visually assessed. DNA methylation-based stemness scores (DNAss) and RNA methylation-based stemness scores (RNAss) were derived from the methylation profiles of each tumor. The correlation between PLIN3 mRNA expression and these scores was then analyzed.<sup>28</sup> Heatmaps were employed to illustrate the relationships between PLIN3 expression and 44 genes involved in N1-methyladenosine (m1A), 5-methylcytosine (m5C), and N6-methyladenosine (m6A) modifications across various cancers.<sup>29</sup>

## Influence of PLIN3 in the Tumor Immune Microenvironment

To enable Gene Set Enrichment Analysis (GSEA), tumor samples were grouped into high and low PLIN3 expression categories according to the median expression levels.<sup>30</sup> The influence of PLIN3 on the tumor microenvironment was assessed by calculating the Immune Score, Stromal Score, ESTIMATE Score, and tumor purity using the “Estimate” package in R.<sup>31</sup> The relationship between PLIN3 levels and six immune subtypes was analyzed using the TISDB Subtype module.<sup>32</sup> Heatmaps were generated to depict correlations between PLIN3 expression and various immune-related genes, including immunostimulatory and immunosuppressive genes, major histocompatibility complex (MHC) molecules, chemokines, and their receptors. The TIMER 2.0 platform was utilized to assess the relationship between PLIN3 levels and immune cell infiltration. Additionally, changes in gene expression in response to anti-PD-L1, and anti-CTLA4 treatments were assessed using the Tumor Immune Syngeneic Mouse (TISMO) web tool.<sup>33</sup> We utilized the SpatialTME database to conduct a comprehensive spatial transcriptomic analysis across various cancers. The SpatialTME database facilitates the deconvolution of the tumor microenvironment (TME) cellular composition.<sup>34</sup> Integration of 10x Visium sequencing data allowed us to construct a pan-cancer spatial transcriptomic atlas. Each microregion in the spatial transcriptomic sections was characterized by the dominant cell types, and the average gene expression within each cell type in every section was examined. We employed the scale function for z-score normalization and visualized the data using the “pheatmap” R package. Furthermore, the spatial distribution and co-localization of PLIN3 with the macrophage markers CD68 and the M2 macrophage marker CD163 were assessed using spatial transcriptomics data from primary lung adenocarcinoma samples (GSM5420751). Deconvolution for this analysis was performed using the “Cottrazm” package. We visualized gene expression landscapes within microregions on 10x Visium slides through the “SpatialFeaturePlot” tool available in the “Seurat” R package.<sup>35</sup> To analyze correlations between cell content across all spots, as well as between cell content and gene expression, we applied Spearman correlation analysis. Visualization of these relationships was accomplished using the “linkET” R package. PLIN3 expression across different immune cells in various cancers was analyzed via the Tumor Immune Single-cell Hub (TISCH).<sup>36</sup> Additionally, the CancerSEA platform’s “correlation plot” module was employed to explore associations between PLIN3 expression and various functional cancer states.<sup>37</sup>

## Multiple Fluorescence Staining

Formalin-fixed, paraffin-embedded tissue sections from lung adenocarcinoma (LUAD) were sourced from Jiangmen Central Hospital. This study was conducted in accordance with the Declaration of Helsinki. All participants provided informed consent, and the study was approved by the hospital's institutional review board (Approval number: 2024–205A). All procedures adhered to relevant guidelines and regulations. Exclusion criteria included patients with autoimmune diseases or those who had received radiotherapy or chemotherapy before surgical tissue collection. Tissue sections were stained with hematoxylin and eosin (Servicebio, China), followed by multi-fluorescence staining of LUAD samples to assess PLIN3 as a marker for M2 macrophages. After deparaffinization and blocking with 5% bovine serum albumin, sections were treated with primary antibodies against PLIN3 (1:500, Proteintech; 10694-1-AP) and either CD163 (1:500, ImmunoWay, YM6146) or CD68 (1:500, ImmunoWay, YM3050). Following secondary antibody application, nuclei were counterstained with DAPI, and the slides were mounted with an antifade medium for confocal imaging (3DHitech Panoramic MIDI). Cellular fluorescence was assessed with Caseviewer software.

## Drug Sensitivity Analysis and Identification of Potential Therapeutics

Cancer cell line (CCL) drug sensitivity data were collated from GDSC,<sup>38</sup> CTRP,<sup>39</sup> and PRISM<sup>40</sup> databases, with AUC values from CTRP and PRISM, and IC50 values from GDSC. Transcriptomic data for CCLs were obtained from the CCLE database.<sup>41</sup> IC50 values were analyzed using the “oncoPredict” R package to correlate PLIN3 expression with drug response metrics. Potential PLIN3-activating compounds were identified using cMap's “query” tool.<sup>42</sup> Molecular docking was initiated by preparing the PLIN3 protein with AutoDock Tools, emphasizing residue repair, hydrogen bond optimization, and energy minimization.<sup>43</sup> The ligands were prepared and minimized using Chem 3D 22.00, followed by virtual screening with AutoDock Vina, and visualization of the results was carried out using Pymol (Educational open source).<sup>44</sup>

## Cell Culture and siRNA-Mediated Gene Silencing

The A549 and H1299 lung cancer cell lines were sourced from the American Type Culture Collection (ATCC). These cell lines were cultured in 1640 medium supplemented with 10% FBS (Servicebio) and 1% penicillin-streptomycin (Meilunbio) at 37°C in a 5% CO<sub>2</sub> incubator (Heal Force). GenePharma (China) supplied the siRNAs targeting PLIN3: siPLIN3#1 with the sequence 5'-GCTGGACAAGTTGGAGGAGAA-3' and siPLIN3#2 with the sequence 5'-GGACAAGTTGGAGGAGAACCT-3'. Cells were transfected with Lipofectamine 2000 (Invitrogen, USA) following the manufacturer's instructions. 48 hours post-transfection, cells were harvested to evaluate PLIN3 knockdown efficiency, as well as cellular proliferation and migration.

## Quantitative Real-Time PCR (RT-PCR)

Total RNA was extracted using the RNAfast200 kit (Fijie Reagent) according to the manufacturer's instructions. Complementary DNA (cDNA) was synthesized and quantitative PCR (qPCR) was performed utilizing Vazyme reagents. GAPDH was used as the internal control. The specific primer sequences and reaction conditions are provided in [Supplementary Table 2](#). Gene expression levels were quantified with the  $2^{-\Delta\Delta C_t}$  method.

## Colony Formation Assay

24 hours post-transfection, A549 and H1299 cells were seeded at a density of 1000 cells per well in 6-well plates and incubated for 7 to 14 days to allow colony formation. The resulting colonies were washed with PBS, fixed using 4% paraformaldehyde for 30 minutes, and subsequently stained with 1% crystal violet for 10 minutes.

## Cell Migration Assay

Migration capabilities of LUAD cells were evaluated using a transwell setup (Corning 3422 with an 8 μm pore size) lacking a Matrigel coating. Briefly described, between 20,000 and 40,000 cells were placed in the upper compartment with 200 μL of serum-free medium. The bottom compartment contained 600 μL of medium enriched with 10% FBS.

After a 24-hour incubation at 37 °C, the chambers were washed with PBS and fixed with 4% paraformaldehyde for about 30 minutes. Cells that did not migrate through the membrane were gently wiped off from the upper side using a cotton swab. Subsequently, the membrane was stained with crystal violet for roughly 30 minutes at ambient temperature, washed with PBS, allowed to air-dry, and subsequently photographed.

## Results

### Expression of PLIN3 in Pan-Cancer Contexts

Figure 1 presents the study's flowchart. Pan-cancer PLIN3 mRNA expression data were obtained from the TCGA and GTEx databases. Notably, PLIN3 expression were found to be elevated in 21 cancer types, including LUAD, liver hepatocellular carcinoma (LIHC), kidney renal clear cell carcinoma (KIRC), and pancreatic adenocarcinoma (PAAD) (Figure 2A). Figures 2B present the differential analysis of paired samples in TCGA. Figure 2C shows the differential analysis of PLIN3 expression in paired tumor and normal tissue samples from TCGA across multiple organs. PLIN3 is notably upregulated in several cancers, including lung, liver, stomach, intestines, thyroid, pancreas, and brain, highlighting its potential as a biomarker and its involvement in lipid metabolism and immune modulation. Further research is needed to clarify its specific roles in these malignancies. It is also highly expressed in reproductive organs like the testes and ovaries, suggesting a function in reproductive tissue biology. PLIN3 demonstrated high diagnostic efficacy, achieving an area under the curve (AUC) greater than 0.7 in predicting 20 cancer types, as illustrated in Figure 2D. Moreover, we validated the upregulation of PLIN3 at the protein level in various cancer types using data from the CPTAC database. Specifically, increases in PLIN3 protein were observed in seven cancer types, including LUAD, PAAD, KIRC, and others. Notably, liver hepatocellular carcinoma (LIHC)

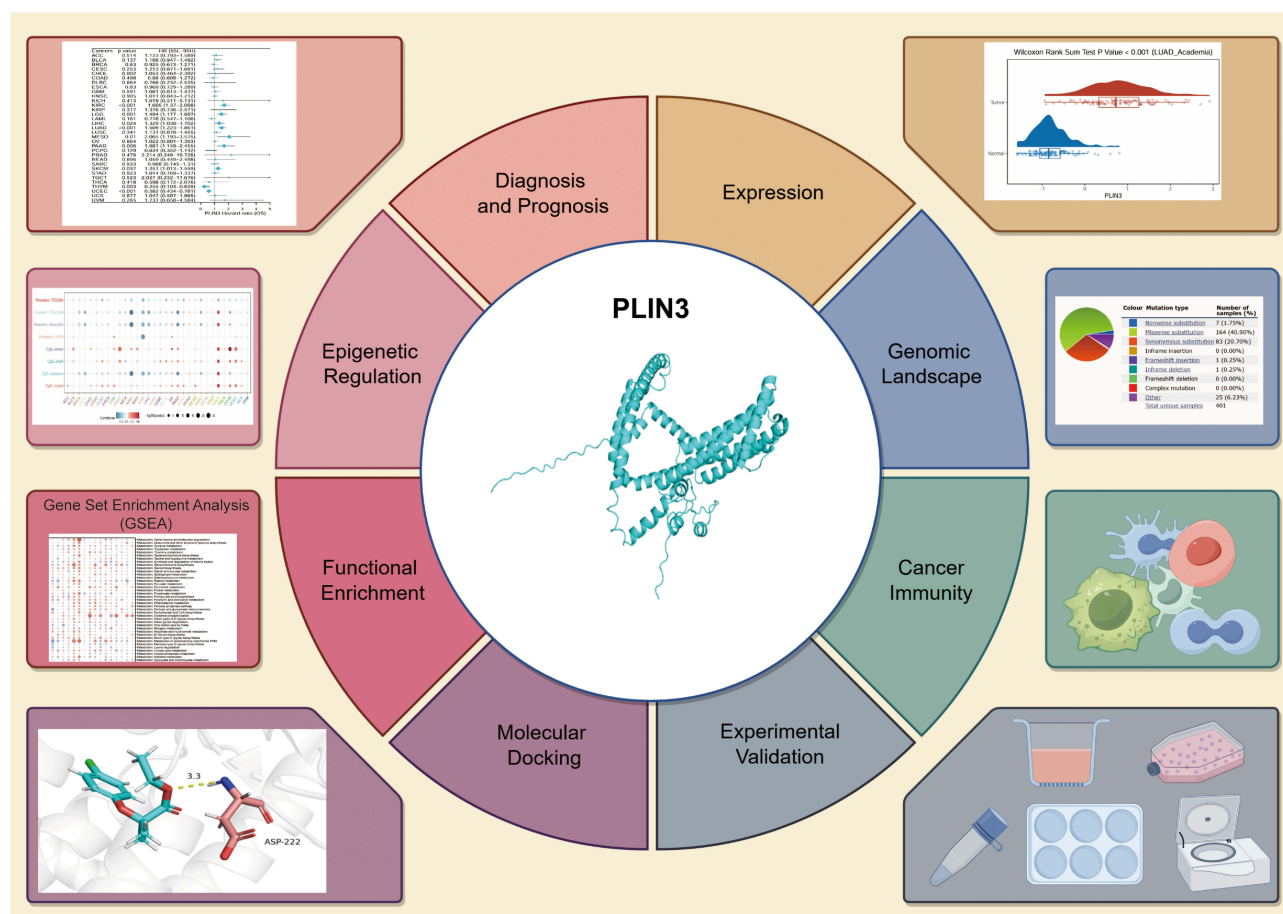
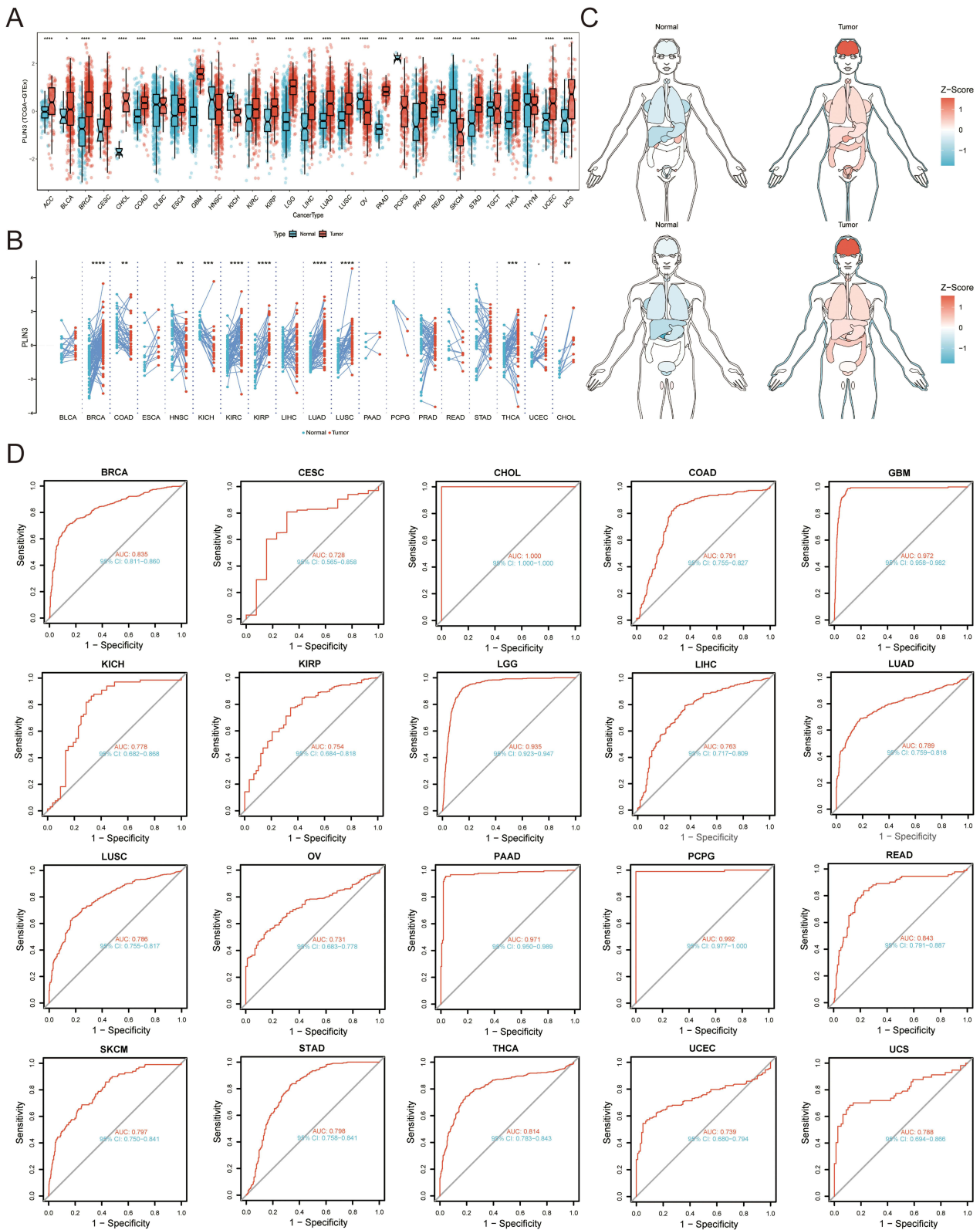


Figure 1 Study flowchart.



**Figure 2** Differential expression of PLIN3 and its prognostic potential across various cancers. **(A)** Comparison of PLIN3 levels in tumor versus normal tissue samples from GTex and TCGA databases. **(B)** PLIN3 mRNA expression in paired tumor and normal samples from TCGA. **(C)** PLIN3 expression profiles across various organs comparing tumor and normal tissues. **(D)** Diagnostic ROC curves evaluating PLIN3 as a biomarker across multiple cancers. Abbreviation list of tumor cohorts from TCGA is given in [Supplementary Table 1](#).

**Notes:** \* $p < 0.05$ , \*\* $p < 0.01$ , \*\*\* $p < 0.001$ , \*\*\*\* $p < 0.0001$ .

**Abbreviations:** TCGA, The Cancer Genome Atlas; GTEx, Genotype-Tissue Expression.

exhibited a contrary expression pattern (Figure 3A). IHC analysis showed strong PLIN3 protein staining in these cancer types, except in LIHC (Figure 3B). Additionally, expression patterns and isoform usage of PLIN3 were analyzed using data from the GEPIA2 database (Supplementary Figure 1A, and B). Furthermore, PLIN3 expression correlated with tumor stages in 12 cancer types, including LUAD and KIRC, suggesting its potential association with cancer progression (Supplementary Figure 2).

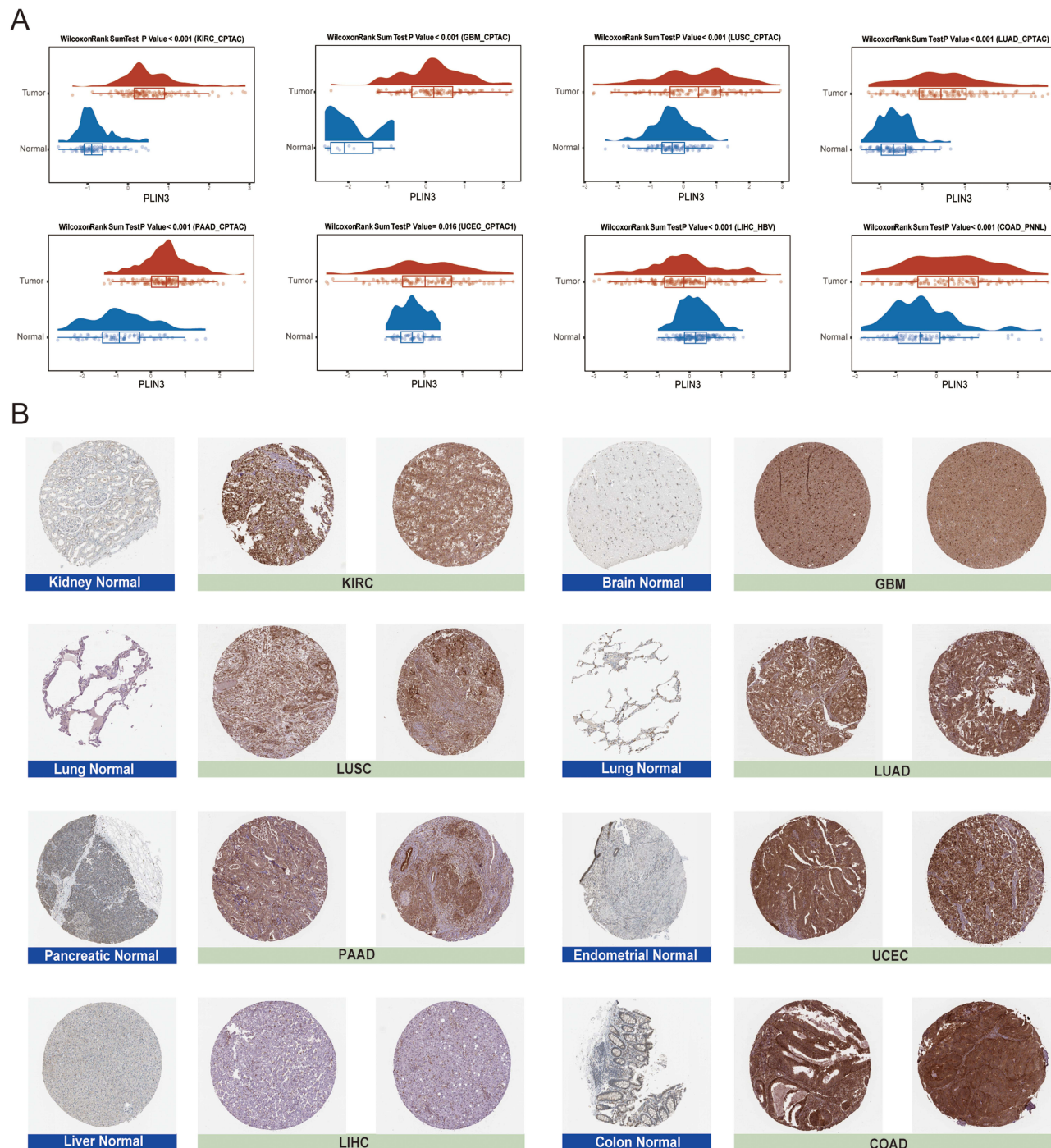


**Figure 3** Differential analysis of PLIN3 protein levels. **(A)** Wilcoxon Rank Sum Tests to compare the statistical differences in expression levels between the tumor and normal groups from the CPTAC dataset. **(B)** IHC images of PLIN3 staining sourced from the Human Protein Atlas. Abbreviation list of tumor cohorts from TCGA is given in Supplementary Table 1.

**Abbreviations:** CPTAC, Clinical Proteomic Tumor Analysis Consortium; IHC, Immunohistochemistry.

# Diagnostic and Prognostic Significance of PLIN3 in Cancer

To assess its prognostic significance, PLIN3 was evaluated as a marker for overall survival (OS), progression-free interval (PFI), disease-free interval (DFI), and disease-specific survival (DSS) across 33 cancer types. Univariate analyses revealed that high PLIN3 levels significantly forecasted OS in KIRC, brain lower grade glioma (LGG), LIHC, LUAD, mesothelioma (MESO), PAAD, and skin cutaneous melanoma (SKCM), while showing a protective impact in thymoma (THYM) and uterine corpus endometrial carcinoma (UCEC) (Figure 4A). Regarding DSS, elevated PLIN3 was associated with increased risk in cancers such as KIRC, LGG, LUAD, and PAAD, yet provided a protective effect in thyroid carcinoma (THCA), THYM, and UCEC (Figure 4B). In terms of DFI, PLIN3 was a risk factor in LGG, cholangiocarcinoma (CHOL), pheochromocytoma and paraganglioma (PCPG), PAAD, and LUAD (Figure 4C).

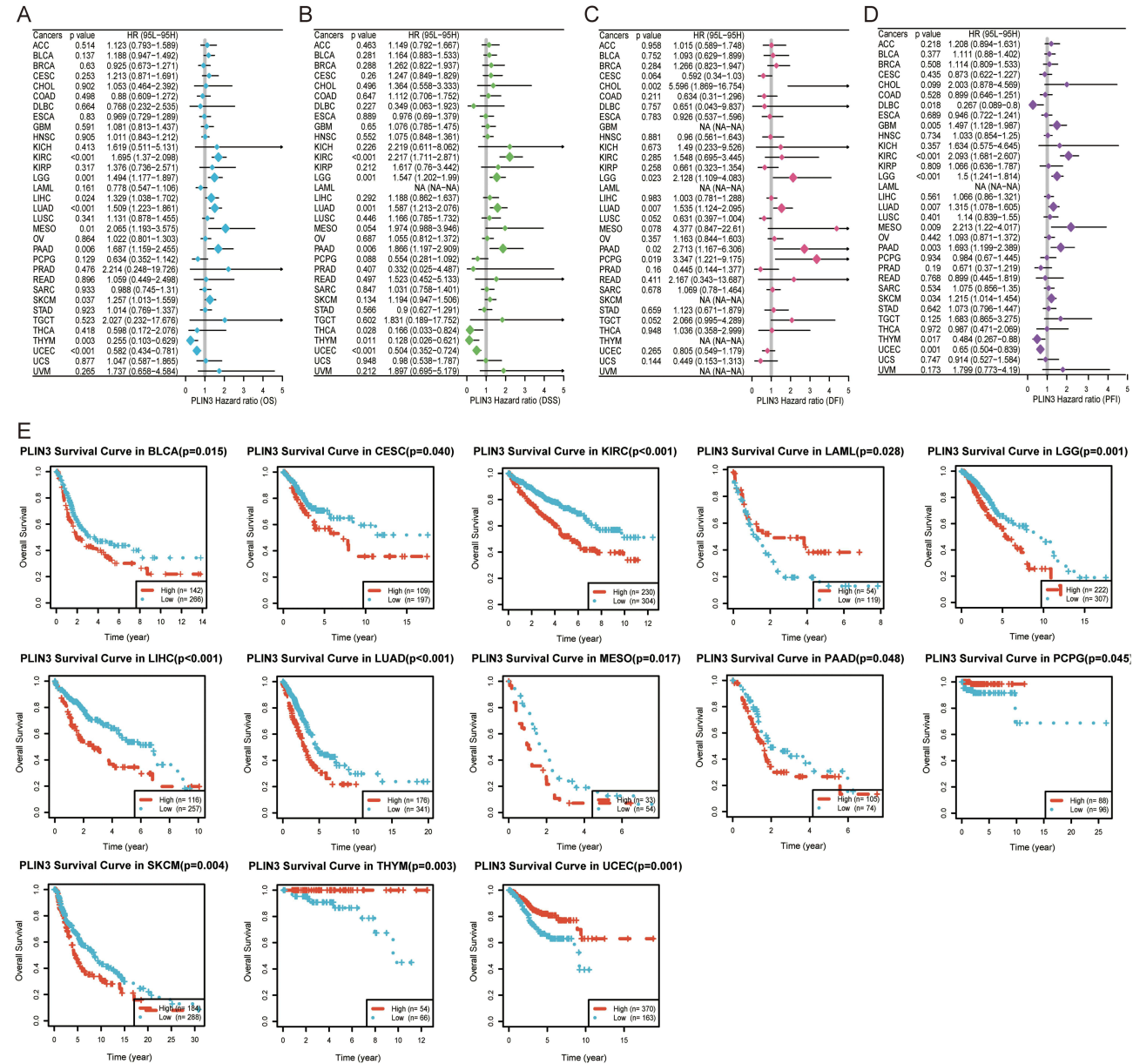


**Figure 4** Survival analysis correlating PLIN3 expression with patient outcomes in pan-cancer. (A–D) Forest plots displaying the prognostic significance of PLIN3 for OS, DSS, DFI, and PFI via univariate Cox regression analysis. (E) Kaplan-Meier plots for OS, with the red and blue lines representing high and low PLIN3 expression groups, respectively. Abbreviation list of tumor cohorts from TCGA is given in Supplementary Table 1.

**Notes:** Log rank tests evaluate differences between survival curves, with p<0.05 indicating statistical significance.

**Abbreviations:** OS, Overall survival; DSS, Disease-specific survival; DFI, Disease-free interval; PFI, Progression-free interval; HR, Hazard ratio.

Similarly, for PFI, PLIN3 was deemed a risk factor in multiple cancers including glioblastoma multiforme (GBM), SKCM, LUAD, MESO, LGG, PAAD, and KIRC, but was protective in lymphoid neoplasm diffuse large B-cell lymphoma (DLBC), THYM, and UCEC (Figure 4D). Kaplan-Meier curves supported these findings, underscoring the complex relationships between PLIN3 levels and cancer prognosis (Figure 4E and [Supplementary Figure 3](#)).

## PLIN3 Genetic Alterations and Genomic Instability Across Cancers

Using the COSMIC database, our study identified missense substitutions as the predominant mutation type in PLIN3, accounting for 40.90% of mutations (Figure 5A). Genetic alterations, which play a crucial role in tumorigenesis, included notable amplifications of PLIN3 in cancers such as LGG and PCPG (Figure 5B). Figure 5C details the locations, types, and frequencies of these PLIN3 alterations. Particularly, the substitution of alanine (A) with valine (V) at position 224 was frequently observed. Somatic copy number alterations (SCNA) were infrequent across the examined cancers; however, a clear pattern emerged showing that higher PLIN3 expression correlated with increased genomic amplification ( $P < 0.001$ , Figure 5D and E). Further analyses explored the impact of PLIN3 on HRD, aneuploidy score, and SNV neoantigens, as well as mutation rates and tumor ploidy, factors crucial for cancer prognosis and treatment response ([Supplementary Figure 4A-F](#)). These findings suggest PLIN3's role in HRD-related pathways and genetic instability, especially in lung cancer, highlighting its potential involvement in cancer development and progression.

## PLIN3 Associations With DNA Repair, Stemness, and Epigenetic Alterations in Pan-Cancer

MMR and homologous recombination repair (HRR) are critical for maintaining genomic integrity.<sup>45</sup> Furthermore, the regulation of stem cell activities is pivotal in cancer progression and in responses to treatment.<sup>46</sup> Our analysis identified strong correlations between PLIN3 and several MMR-related genes across 22 cancer types, including LUAD, PAAD, and LIHC ( $P < 0.05$ , Figure 6A). Additionally, PLIN3 was positively associated with DNAss in UVM, and RNAss in ACC ( $P < 0.05$ , Figures 6B, C). We further explored epigenetic modifications of PLIN3 across various cancers. A heatmap detailed the relationship between methylation levels at different genomic regions associated with the PLIN3 gene, including the promoter, untranslated regions, and CpG contexts such as islands, shores, shelves, and open sea areas ([Supplementary Figure 5](#)). Methylation in promoter-related regions of PLIN3 inversely correlated with its mRNA expression in most cancers. The analysis also evaluated the relationships between PLIN3 and four key methyltransferases—DNMT1, DNMT2, DNMT3A, DNMT3B—revealing significant correlations in cancers such as PAAD, LIHC, and KIRC (Figure 6E). Further investigation into the associations between PLIN3 and 44 regulators of RNA modifications showed positive associations with m1A, m5C, and m6A methylation across most cancer types (Figure 6D). These findings highlight the extensive involvement of PLIN3 in regulating DNA and RNA modifications, potentially impacting genomic stability and influencing the pathophysiology of various cancers.

## PLIN3 Is Involved in Cancer Immune Pathways in LUAD

The ESTIMATE algorithm was employed to investigate the relationship between PLIN3 and the TME, calculating the ImmuneScore, StromalScore, and ESTIMATEScore in pan-cancer. A positive correlation was identified between PLIN3 and the ImmuneScore in 13 cancer types, including KIRC, PAAD, LIHC, and LUAD (Figure 6H). These findings align with the GSEA results, suggesting that PLIN3 may enhance cellular infiltration in these cancers, potentially influencing the response to immunotherapy.

Further analysis was performed to investigate the distribution of immune subtypes based on PLIN3 expression levels, revealing a predominance of the C2 subtype in the high PLIN3 group and the C3 subtype in the low PLIN3 group ([Supplementary Figure 6](#)). This suggests that high PLIN3 expression may be associated with a more active immune response, which could have implications for immunotherapy efficacy. Using the TISMO tool, we compared PLIN3 gene expression across various tumor models and immune checkpoint blockade (ICB) treatments, as well as between pre- and post-ICB treatment in both responders and non-responders ([Supplementary Figure 7](#)). The correlations between PLIN3 expression and significant biomarkers for immunotherapy, such as TMB and MSI, were assessed. We observed a positive



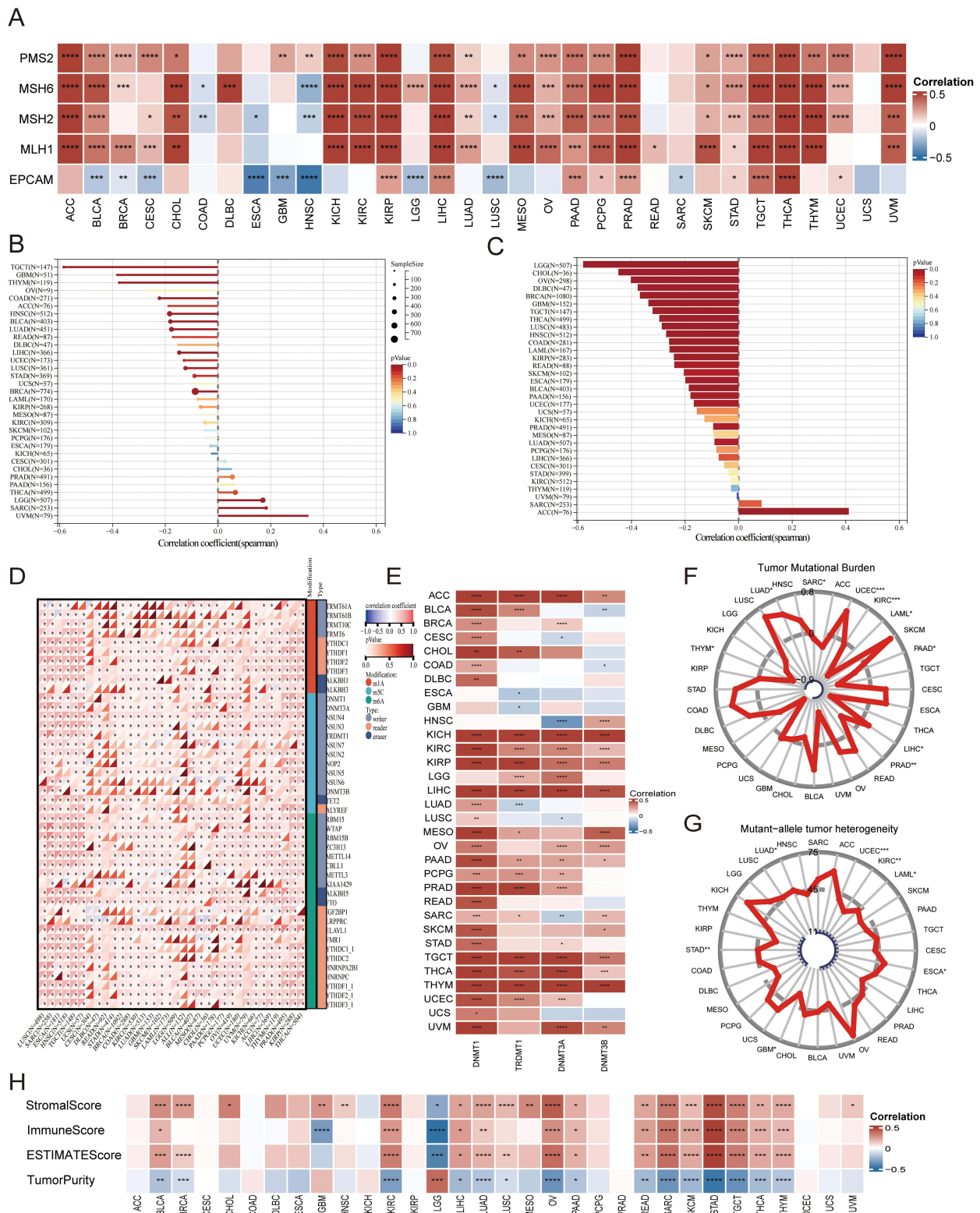


**Figure 6** Associations of PLIN3 with DNA repair, stemness, and epigenetic modifications. **(A)** Heatmap illustrating correlations between PLIN3 and five MMR-related genes. **(B)** Lollipop chart detailing the correlation of PLIN3 levels with DNA methylation-based stem scores. **(C)** Bar chart showing the correlation of PLIN3 levels with RNA methylation-based stem scores. **(D)** Heatmap of the relationships between PLIN3 levels and RNA modifications. **(E)** Heatmap displaying associations of PLIN3 with four methyltransferases. **(F)** Radar chart presenting the Spearman correlation between PLIN3 expression levels and TMB across pan-cancer. **(G)** Radar chart showing the Spearman correlation between PLIN3 expression levels and MSI across pan-cancer. **(H)** Heatmap displaying relationships between PLIN3 expression and ESTIMATE, Immune, and Stromal scores, with statistical significance indicated as \* $p < 0.05$ , \*\* $p < 0.01$ , \*\*\* $p < 0.001$ , \*\*\*\* $p < 0.0001$ . Abbreviation list of tumor cohorts from TCGA is given in [Supplementary Table 1](#). **Abbreviations:** m1A, N1-methyladenosine; m5c, 5-methylcytosine; m6a, N6-methyladenosine; MMR, mismatch repair; TMB, Tumor mutation burden; MSI, Microsatellite instability.

To gain deeper insights into the effect of PLIN3 on tumor prognosis, we performed a pan-cancer GSEA. This analysis involved comparing the differentially expressed genes in patients with high versus low PLIN3 expression across various cancer types. The heatmap analysis revealed notable enrichment of immune-related pathways, such as interferon-gamma, interferon-alpha, inflammatory, interleukin-6, and interleukin-2, suggesting a role for PLIN3 in the antitumor immune response (Figure 7). Furthermore, high PLIN3 expression was positively correlated with epithelial-mesenchymal transition (EMT) in LUAD, BLCA, and KIRC patients. This correlation may underlie the tendency for patients with elevated PLIN3 levels in these cancers to experience lymph node and distant metastasis, as well as recurrence. Additionally, PLIN3 was found to be closely linked with multiple lipid metabolism pathways, which may relate to the functionality of immune cells such as macrophages. These cells accumulate lipid droplets within the tumor microenvironment, potentially affecting their polarization and function, thereby influencing inflammatory responses and tumor cell clearance. Moreover, PLIN3 is involved in drug metabolism processes, possibly affecting responses to chemotherapy.

To investigate which immune cell types might be influenced by PLIN3 expression across cancers, we used seven different algorithms to analyze correlations, ensuring the accuracy of our results through cross-validation. As depicted in Figure 8B, PLIN3 expression was positively correlated with the infiltration of cancer-associated fibroblasts, macrophages, and neutrophils. We also examined the relationships between PLIN3 and immune-related genes that encode immunosuppressive and activating proteins, as well as chemokines, their receptors, and MHC proteins (Figure 8A). Notably, high PLIN3 expression levels correlated positively with various immune-related molecules across a broad spectrum of cancers, further supporting its role in modulating the immune microenvironment.

## PLIN3 Expression as a Key Marker of M2 Macrophage Infiltration

To gain a deeper understanding of which cell types express PLIN3 in tumor tissues, we examined 162 slices from spatial transcriptomes. We observed prominent PLIN3 expression predominantly in tumor cells and macrophage-rich microregions (Figure 9A). Spatial transcriptomic analysis highlighted strong co-localization of PLIN3 with the macrophage markers CD68 and CD163 in LUAD, with a substantial positive correlation between PLIN3 levels and macrophage presence in these spots (Figure 9B and C). Furthermore, the single-cell expression profiles of PLIN3, based on 68 datasets from the TISCH database, showcased extensive expression across various cancers, particularly in monocytes/macrophages and malignant cells, as depicted in the heatmap (Figure 9D). UMAP analysis demonstrated pronounced PLIN3 expression, particularly in macrophages within non-small cell lung cancer (NSCLC, EMTAB6149) and kidney renal clear cell carcinoma (KIRC, GSE159115) (Figures 9E and F). Supporting these findings, fluorescent staining demonstrated the co-expression of PLIN3 with both CD68 and CD163 in LUAD tissue sections (Figures 10A and B). Collectively, the data from bulk, spatial, single-cell transcriptomic analyses, and fluorescence staining establish a strong correlation between PLIN3 expression and M2 macrophage infiltration, highlighting the potential of PLIN3 as a biomarker for M2 macrophage presence across various cancers.

## Potential Role of PLIN3 in LUAD Cells

To further investigate the functional role of PLIN3 in tumor cells, we generated stable PLIN3-knockdown cells using the A549 and H1299 LUAD cell lines. The efficacy of the PLIN3 knockdown was verified via RT-QPCR (Figure 10C). Colony formation assays confirmed that knocking down PLIN3 significantly reduced the colony-forming ability of A549 and H1299 cells (Figure 10D). Furthermore, transwell assays showed that silencing PLIN3 hindered the migratory capacity of A549 and H1299 cells (Figure 10E). CancerSEA single-cell sequencing data were analyzed to assess the relationship between PLIN3 expression and 14 functional states of cancer. The results revealed strong positive correlations with various cancer-related processes, including angiogenesis, apoptosis, EMT, hypoxia, inflammation, invasion, metastasis, and quiescence in LUAD (Supplementary Figure 8).

## Drug Sensitivity Analysis

In pan-cancer analyses, the “cor.test” function was employed to ascertain the Spearman correlation between PLIN3 and various chemotherapy drugs across multiple databases (Figure 11A). The results indicated that PLIN3 could potentially be sensitive to chemotherapy. To further explore potential therapeutic strategies to counteract the tumorigenic effects



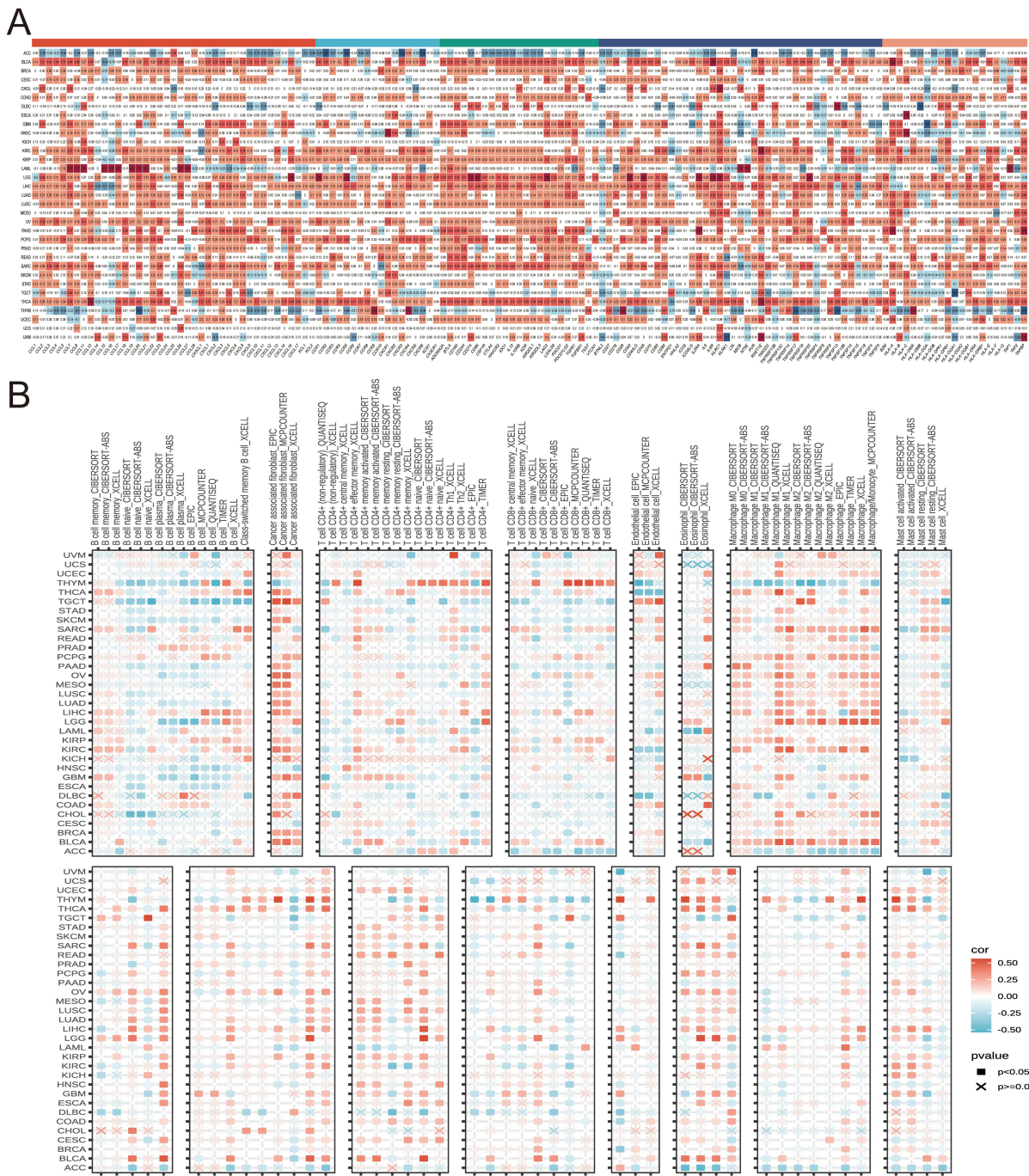


**Figure 8** Correlation analysis between PLIN3 expression and immune cell infiltration. **(A)** Heatmap showing correlations between PLIN3 mRNA expression and the expression of chemokines, chemokine receptors, immune-inhibitors, immune-stimulatory, and MHC genes. **(B)** Heatmaps displaying correlations between PLIN3 expression and infiltration levels of various immune cells. Abbreviation list of tumor cohorts from TCGA is given in [Supplementary Table 1](#). Abbreviations: MHC, Major histocompatibility complex.

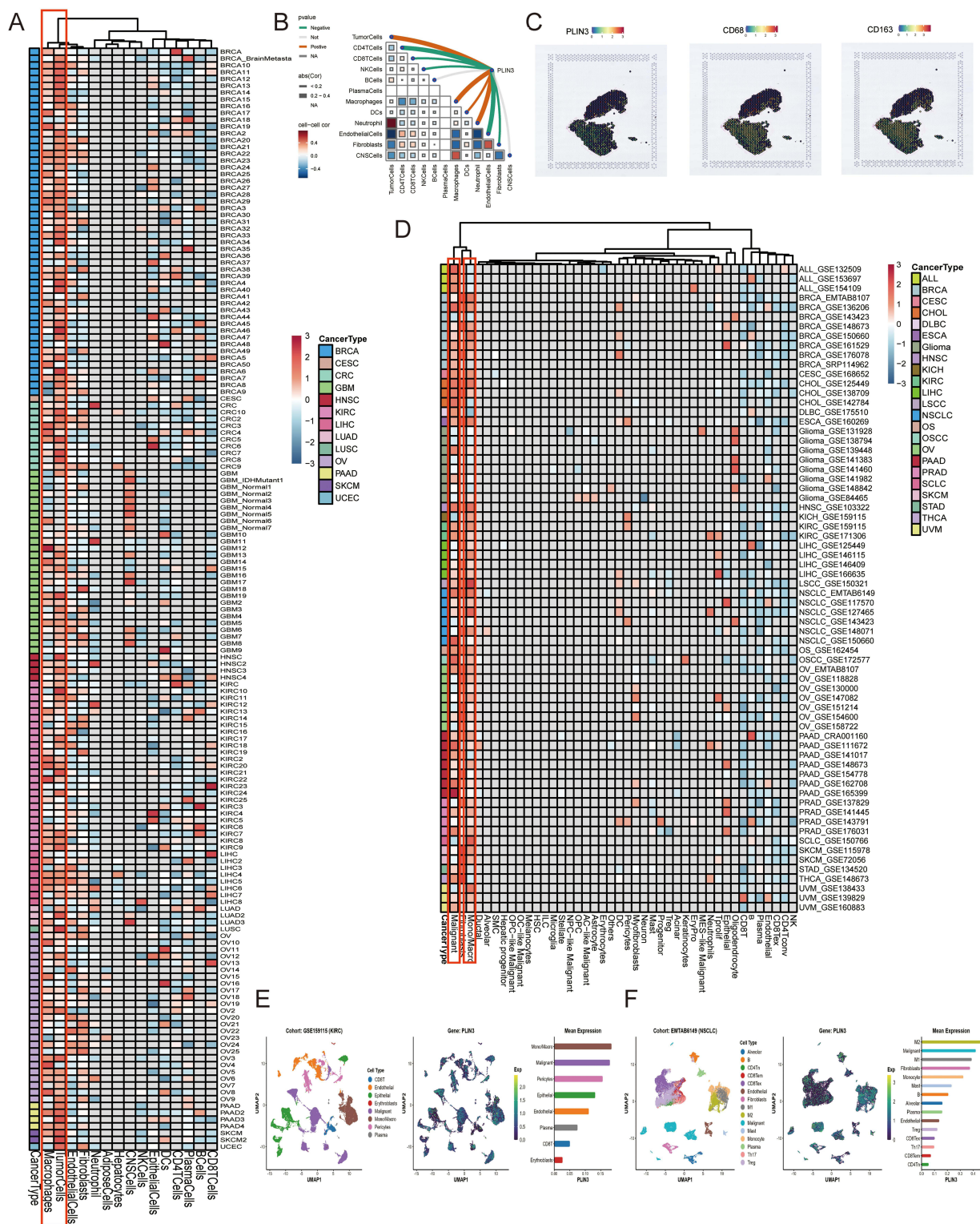


**Figure 9** PLIN3 as a Potential Marker of M2 Macrophage Infiltration. **(A)** Heatmap showing PLIN3 gene expression across various microdomains in pan-cancer spatial transcriptomic sections. Rows represent different datasets, each labeled in a color specific to the disease type. Columns represent different cell types, with the color intensity on the right scale indicating data values—darker red signifies higher values, and lighter colors indicate lower values. Gray indicates that the cell type is absent in the microregion. The red boxes highlight PLIN3's widespread expression in macrophage and malignant cell types. **(B)** Spearman correlation analysis used to calculate the correlation between cell content across all spots and between cell content and gene expression levels. Red lines indicate positive correlations, green lines indicate negative correlations, and gray lines indicate non-significant correlations. Line thickness represents the magnitude of the correlation coefficient **(C)** Spatial transcriptomics exploring co-localization patterns of PLIN3 with CD68 and CD163, color-coded by expression levels. Each dot represents a microdomain (spot) with deeper red indicating higher gene expression. **(D)** Expression of PLIN3 in cancer-specific single-cell clusters analyzed using the TISCH database. The red boxes highlight PLIN3's widespread expression in monocyte, macrophage and malignant cell types. **(E-F)** UMAP plots detailing cell type distributions and PLIN3 intensity in KIRC **(E)** and NSCLC **(F)**. Abbreviation list of tumor cohorts from TCGA is given in [Supplementary Table 1](#). **Abbreviations:** TISCH, Tumor Immune Single-cell Hub; NSCLC, non-small cell lung cancer.

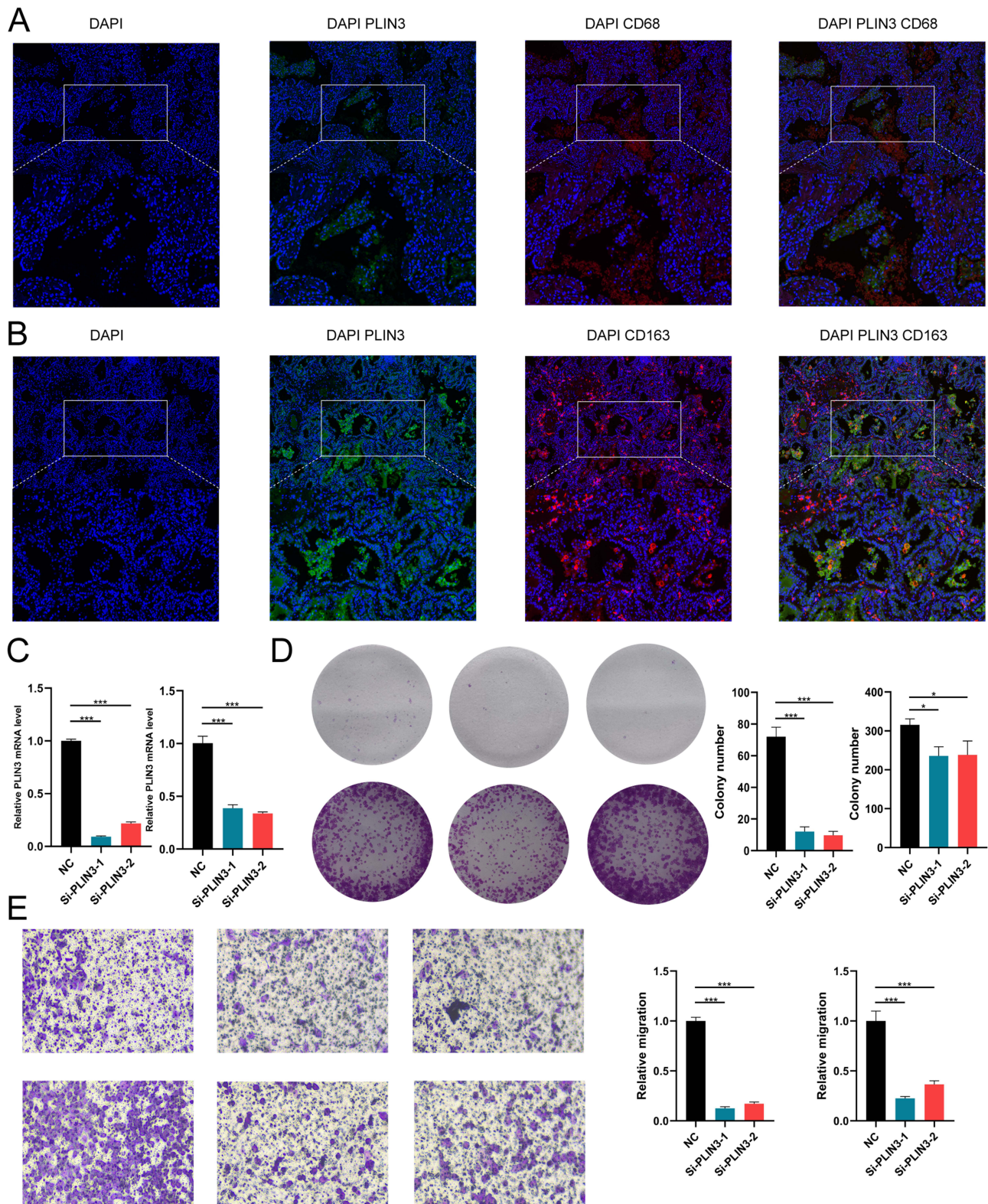


**Figure 10** Investigation of PLIN3's role in regulating malignancy in LUAD tumor cells. **(A)** Fluorescent staining of tumor tissues showing CD68 (red) and PLIN3 (green), with DAPI (blue) for counterstaining. **(B)** Fluorescent images of tumor tissues with CD163 (red) and PLIN3 (green), counterstained with DAPI (blue). **(C)** PLIN3 mRNA expression levels in transfected cells. **(D)** Colony formation assay to evaluate the impact of PLIN3 on tumor cell proliferation. **(E)** Wound healing assay assessing the effect of PLIN3 knockdown on tumor cell migration.

**Notes:** Statistical significance is indicated by \* $p < 0.05$ , \*\*\* $P < 0.001$ .

**Abbreviations:** LUAD, Lung adenocarcinoma.



associated with PLIN3, we conducted a Connectivity Map (CMap) analysis. A PLIN3-related signature was developed, comprising 150 genes that were significantly upregulated and 150 genes that were significantly downregulated, identified by screening patients with high and low PLIN3 expression across various cancers. Using the Extreme Summarization (XSum) method, we compared PLIN3-related traits with CMap gene signatures, resulting in similarity scores for 1288 compounds. Compounds such as clofibrate, PHA.00816795, X4.5. dianilinophthalimide, and exisulind displayed relatively lower scores across most cancers, indicating their potential to counteract PLIN3-mediated carcinogenic effects (Figure 11B). Further CMap analysis specifically for LUAD identified clofibrate as a compound capable of potentially reversing PLIN3's dysregulated molecular traits and mitigating its oncogenic effects (Figure 11C). To evaluate the potential interaction between the PLIN3 protein and clofibrate, molecular docking analysis was conducted. Ten PLIN3 models were generated using AlphaFold2.0, based on the provided FASTA sequence (Supplementary Material 1). The top-ranked model exhibited an overall quality factor of 87.84. AutoDock Vina 1.05.36 successfully docked W.13 to PLIN3 (DockScore:  $-3.564$  kcal/mol) (Figure 11D), indicating the potential of clofibrate to modulate PLIN3 activity. These results provide substantial support for our predictions, though further studies are necessary to clarify the mechanisms involved.

## Discussion

Over the past decade, immunotherapy has significantly extended the survival of patients with advanced tumors, revolutionizing clinical treatment strategies.<sup>47</sup> However, its effectiveness is restricted to a specific subset of patients, mainly due to the heterogeneity within the tumor-immune microenvironment.<sup>4</sup> Identifying predictors of clinical response to immunotherapy could enhance the selection of suitable tumor types and patient subgroups. In this study, multi-omics approaches integrating data from various platforms revealed that PLIN3 may serve as a novel immunological marker, influencing macrophage infiltration and promote tumor proliferation and migration, suggesting its potential in guiding immunotherapy decisions.

Initially, we quantified PLIN3 mRNA and protein levels in tumor tissues compared to normal tissues across various cancers. Our findings indicate a consistent overexpression of PLIN3 in multiple cancer types. ROC analysis further validated these findings with high confidence. Further investigation into PLIN3's prognostic potential, considering OS, DSS, DFI, and PFI, revealed significant correlations. Elevated PLIN3 levels were linked to a higher risk and worse outcomes in several cancers, including KIRC, LGG, LIHC, LUAD, MESO, PAAD, and SKCM. Conversely, high PLIN3 expression was associated with better prognosis in THYM and UCEC, suggesting a protective role in these contexts. We further explored the relationship between PLIN3 expression levels and clinical features across these cancers. Aligning with our survival outcomes, high PLIN3 expression was related to lower TNM stages in THYM and UCEC. Conversely, in KIRC and LUAD, elevated PLIN3 levels correlated with an increased risk of metastasis and disease progression, as confirmed by GESA and *in vitro* cellular assays, underscoring PLIN3 as a prognostic biomarker.

Our analysis also explored PLIN3's role in the immune landscape of tumors. We discovered that PLIN3 expression correlates with the immune score, suggesting its role in influencing the tumor microenvironment. Immune infiltration analyses further demonstrated a significant positive association between PLIN3 and the expression of MHC, immune inhibitors, immune stimulators, and chemokine genes. Utilizing seven different algorithms, we found a consistent positive relationship between PLIN3 mRNA levels and M2 macrophage presence across various cancers. These findings were substantiated by both bulk and single-cell transcriptomic as well as spatial transcriptomic sequencing data, revealing co-expression patterns between PLIN3 and M2 macrophage markers.

TMB is recognized as an effective predictor of responses to ICB therapy, with several studies documenting its association with treatment response and survival benefits.<sup>48,49</sup> MSI, indicative of genetic instability, is increasingly used to select patients likely to benefit from immunotherapy, targeted treatments, and comprehensive systemic therapies.<sup>50</sup> Patients with high TMB or MSI levels often experience improved long-term survival outcomes following immunotherapy.<sup>51,52</sup> To our knowledge, the association between PLIN3 and TMB or MSI has not been previously explored. Our study examined this relationship in LUAD, finding a positive relationship between PLIN3 expression and both MSI and TMB levels. This suggests that PLIN3 could impact the effectiveness of immunotherapy in LUAD patients.

In our CMap analysis, we identified four compounds—exisulind, X4.5.dianilinophthalimide, PHA.00816795, and clofibrate—as potential inhibitors of PLIN3-mediated pro-oncogenic activities. Exisulind, a phosphodiesterase 5 (PDE5) inhibitor, demonstrates antitumor properties by boosting cGMP levels, which activate protein kinase G (PKG) and promote apoptosis.<sup>53</sup> This compound disrupts critical signaling pathways including  $\beta$ -catenin degradation and MAPK/JNK, leading to growth arrest in multiple cancers such as breast, lung, prostate, and colon.<sup>54,55</sup> Similarly, clofibrate, a PPAR- $\alpha$  agonist, displays anticancer activity by causing cell cycle arrest, enhancing apoptosis, and inhibiting inflammatory pathways such as NF- $\kappa$ B and ERK1/2.<sup>56</sup> It also diminishes lipogenic and proliferative signaling, enhances sensitivity to radio- and chemotherapy, and stimulates autophagy, making it effective against breast, pancreatic, liver, and colorectal cancers.<sup>57–60</sup> These findings contribute novel perspectives for future research on PLIN3's role in cancer development and progression.

## Conclusions

In conclusion, our multi-omics pan-cancer analysis identifies PLIN3 as a key marker of cancer prognosis and immunity, strongly linked to M2 macrophage infiltration across various cancer types. This study highlights PLIN3's role in tumor progression and suggests potential therapeutic strategies, including the use of compounds like clofibrate. By deepening our understanding of PLIN3's function, these findings open up promising treatment options for patients with limited therapeutic responses.

## Data Sharing Statement

The original contributions presented in the study are included in the article/[Supplementary Materials](#). Further inquiries can be directed to the corresponding authors.

## Ethical Statement

The studies involving human participants were reviewed and approved by The Clinical Research Ethics Committee of Jiangmen Central Hospital (Approval number: 2024-205A).

## Acknowledgments

Shaohua Yang, Hejie Liu, and Youbin Zheng are co-first authors for this study. The schematic diagram of the graphical abstract was drawn by Figdraw.

## Funding

This work was supported by the Technology Project of Jiangmen (Nos. 2220002000183, 2320002000933), the Medical Science Foundation of Jiangmen Central Hospital (J202401), and Guangdong Province Basic and Applied Basic Research Fund (2023A1515140028).

## Disclosure

All authors report no competing interests in this work.

## References

1. Sung H, Ferlay J, Siegel RL, et al. Global Cancer Statistics 2020: GLOBOCAN estimates of incidence and mortality worldwide for 36 cancers in 185 countries. *CA Cancer J Clin.* 2021;71(3):209–249. doi:10.3322/caac.21660
2. Srivastava S, Koay EJ, Borowsky AD, et al. Cancer overdiagnosis: a biological challenge and clinical dilemma. *Nat Rev Cancer.* 2019;19(6):349–358. doi:10.1038/s41568-019-0142-8
3. Vargas AJ, Harris CC. Biomarker development in the precision medicine era: lung cancer as a case study. *Nat Rev Cancer.* 2016;16(8):525–537. doi:10.1038/nrc.2016.56
4. Xu S, Chen X, Ying H, et al. Multi-omics identification of a signature based on malignant cell-associated ligand-receptor genes for lung adenocarcinoma. *BMC Cancer.* 2024;24(1):1138. doi:10.1186/s12885-024-12911-5
5. Mantovani A, Marchesi F, Malesci A, Laghi L, Allavena P. Tumour-associated macrophages as treatment targets in oncology. *Nat Rev Clin Oncol.* 2017;14(7):399–416. doi:10.1038/nrclinonc.2016.217
6. Qian BZ, Pollard JW. Macrophage diversity enhances tumor progression and metastasis. *Cell.* 2010;141(1):39–51. doi:10.1016/j.cell.2010.03.014

7. Zhang QW, Liu L, Gong CY, et al. Prognostic significance of tumor-associated macrophages in solid tumor: a meta-analysis of the literature. *PLoS One*. 2012;7(12):e50946. doi:10.1371/journal.pone.0050946
8. Straub BK, Herpel E, Singer S, et al. Lipid droplet-associated PAT-proteins show frequent and differential expression in neoplastic steatogenesis. *Mod Pathol*. 2010;23(3):480–492. doi:10.1038/modpathol.2009.191
9. Gu Y, Yang Y, Cao X, et al. Plin3 protects against alcoholic liver injury by facilitating lipid export from the endoplasmic reticulum. *J Cell Biochem*. 2019;120(9):16075–16087. doi:10.1002/jcb.28889
10. Lamprou I, Tsolou A, Kakouratos C, et al. Suppressed PLIN3 frequently occurs in prostate cancer, promoting docetaxel resistance via intensified autophagy, an event reversed by chloroquine. *Med Oncol*. 2021;38(10):116. doi:10.1007/s12032-021-01566-y
11. Varela LM, López S, Ortega-Gómez A, et al. Postprandial triglyceride-rich lipoproteins regulate perilipin-2 and perilipin-3 lipid-droplet-associated proteins in macrophages. *J Nutr Biochem*. 2015;26(4):327–336. doi:10.1016/j.jnutbio.2014.11.007
12. Gu JQ, Wang DF, Yan XG, et al. A Toll-like receptor 9-mediated pathway stimulates perilipin 3 (TIP47) expression and induces lipid accumulation in macrophages. *Am J Physiol Endocrinol Metab*. 2010;299(4):E593–600. doi:10.1152/ajpendo.00159.2010
13. He Y, Liu L, Dong Y, et al. Lipid droplets-related Perilipin-3: potential immune checkpoint and oncogene in oral squamous cell carcinoma. *Cancer Immunol Immunother*. 2024;73(5):78. doi:10.1007/s00262-024-03659-9
14. Lamprou I, Kakouratos C, Tsolou A, et al. Lipophagy-related protein perilipin-3 and resistance of prostate cancer to radiation therapy. *Int J Radiat Oncol Biol Phys*. 2022;113(2):401–414. doi:10.1016/j.ijrobp.2022.01.033
15. Zhou L, Song Z, Hu J, et al. ACS3 represses prostate cancer progression through downregulating lipid droplet-associated protein PLIN3. *Theranostics*. 2021;11(2):841–860. doi:10.7150/thno.49384
16. Wang K, Ruan H, Song Z, et al. PLIN3 is up-regulated and correlates with poor prognosis in clear cell renal cell carcinoma. *Urol Oncol*. 2018;36(7):343.e9–343.e19. doi:10.1016/j.urolonc.2018.04.006
17. Than GN, Turóczy T, Sümegi B, et al. Overexpression of placental tissue protein 17b/TIP47 in cervical dysplasias and cervical carcinoma. *Anticancer Res*. 2001;21(1b):639–642.
18. Wu YJ, Wang J, Zhang P, et al. PIWIL1 interacting RNA piR-017724 inhibits proliferation, invasion, and migration, and inhibits the development of HCC by silencing PLIN3. *Front Oncol*. 2023;13:1203821. doi:10.3389/fonc.2023.1203821
19. Xu S, Zheng Y, Ye M, et al. Comprehensive pan-cancer analysis reveals EPHB2 is a novel predictive biomarker for prognosis and immunotherapy response. *BMC Cancer*. 2024;24(1):1064. doi:10.1186/s12885-024-12843-0
20. Goldman MJ, Craft B, Hastie M, et al. Visualizing and interpreting cancer genomics data via the Xena platform. *Nat Biotechnol*. 2020;38(6):675–678. doi:10.1038/s41587-020-0546-8
21. Pontén F, Jirstrom K, Uhlen M. The Human Protein Atlas—a tool for pathology. *J Pathol*. 2008;216(4):387–393. doi:10.1002/path.2440
22. Cerami E, Gao J, Dogrusoz U, et al. The cBio cancer genomics portal: an open platform for exploring multidimensional cancer genomics data. *Cancer Discov*. 2012;2(5):401–404. doi:10.1158/2159-8290.Cd-12-0095
23. Ritchie ME, Phipson B, Wu D, et al. limma powers differential expression analyses for RNA-sequencing and microarray studies. *Nucleic Acids Res*. 2015;43(7):e47. doi:10.1093/nar/gkv007
24. Chandrashekar DS, Karthikeyan SK, Korla PK, et al. UALCAN: an update to the integrated cancer data analysis platform. *Neoplasia*. 2022;25:18–27. doi:10.1016/j.neo.2022.01.001
25. Thorsson V, Gibbs DL, Brown SD, et al. The immune landscape of cancer. *Immunity*. 2018;48(4):812–830.e14. doi:10.1016/j.immuni.2018.03.023
26. Latham A, Srinivasan P, Kemel Y, et al. Microsatellite instability is associated with the presence of lynch syndrome pan-cancer. *J Clin Oncol*. 2019;37(4):286–295. doi:10.1200/jco.18.00283
27. Lyko F. The DNA methyltransferase family: a versatile toolkit for epigenetic regulation. *Nat Rev Genet*. 2018;19(2):81–92. doi:10.1038/nrg.2017.80
28. Malta TM, Sokolov A, Gentles AJ, et al. Machine learning identifies stemness features associated with oncogenic dedifferentiation. *Cell*. 2018;173(2):338–354.e15. doi:10.1016/j.cell.2018.03.034
29. Shi H, Chai P, Jia R, Fan X. Novel insight into the regulatory roles of diverse RNA modifications: re-defining the bridge between transcription and translation. *mol Cancer*. 2020;19(1):78. doi:10.1186/s12943-020-01194-6
30. Liberzon A, Birger C, Thorvaldsdóttir H, Ghandi M, Mesirov JP, Tamayo P. The Molecular Signatures Database (MSigDB) hallmark gene set collection. *Cell Syst*. 2015;1(6):417–425. doi:10.1016/j.cels.2015.12.004
31. Yoshihara K, Shahmoradgoli M, Martínez E, et al. Inferring tumour purity and stromal and immune cell admixture from expression data. *Nat Commun*. 2013;4(1):2612. doi:10.1038/ncomms3612
32. Wan J, Qian SB. TISdb: a database for alternative translation initiation in mammalian cells. *Nucleic Acids Res*. 2014;42(Database issue):D845–50. doi:10.1093/nar/gkt1085
33. Zeng Z, Wong CJ, Yang L, et al. TISMO: syngeneic mouse tumor database to model tumor immunity and immunotherapy response. *Nucleic Acids Res*. 2022;50(D1):D1391–d1397. doi:10.1093/nar/gkab804
34. Shi J, Wei X, Xun Z, et al. The web-based portal SpatialTME integrates histological images with single-cell and spatial transcriptomics to explore the tumor microenvironment. *Cancer Res*. 2024;84(8):1210–1220. doi:10.1158/0008-5472.Can-23-2650
35. Xun Z, Ding X, Zhang Y, et al. Reconstruction of the tumor spatial microenvironment along the malignant-boundary-nonmalignant axis. *Nat Commun*. 2023;14(1):933. doi:10.1038/s41467-023-36560-7
36. Sun D, Wang J, Han Y, et al. TISCH: a comprehensive web resource enabling interactive single-cell transcriptome visualization of tumor microenvironment. *Nucleic Acids Res*. 2021;49(D1):D1420–d1430. doi:10.1093/nar/gkaa1020.
37. Yuan H, Yan M, Zhang G, et al. CancerSEA: a cancer single-cell state atlas. *Nucleic Acids Res*. 2019;47(D1):D900–d908. doi:10.1093/nar/gky939.
38. Yang W, Soares J, Greninger P, et al. Genomics of Drug Sensitivity in Cancer (GDSC): a resource for therapeutic biomarker discovery in cancer cells. *Nucleic Acids Res*. 2013;41(Database issue):D955–61. doi:10.1093/nar/gks1111
39. Basu A, Bodycombe NE, Cheah JH, et al. An interactive resource to identify cancer genetic and lineage dependencies targeted by small molecules. *Cell*. 2013;154(5):1151–1161. doi:10.1016/j.cell.2013.08.003
40. Yu C, Mannan AM, Yvone GM, et al. High-throughput identification of genotype-specific cancer vulnerabilities in mixtures of barcoded tumor cell lines. *Nat Biotechnol*. 2016;34(4):419–423. doi:10.1038/nbt.3460

41. Barretina J, Caponigro G, Stransky N, et al. The cancer cell line encyclopedia enables predictive modelling of anticancer drug sensitivity. *Nature*. 2012;483:7391):603–7. doi:10.1038/nature11003
42. Subramanian A, Narayan R, Corsello SM, et al. A next generation connectivity map: 11000 platform and the first 1,000,000 profiles. *Cell*. 2017;171(6):1437–1452.e17. doi:10.1016/j.cell.2017.10.049
43. Morris GM, Huey R, Lindstrom W, et al. AutoDock4 and AutoDockTools4: automated docking with selective receptor flexibility. *J Comput Chem*. 2009;30(16):2785–2791. doi:10.1002/jcc.21256
44. Trott O, Olson AJ. AutoDock Vina: improving the speed and accuracy of docking with a new scoring function, efficient optimization, and multithreading. *J Comput Chem*. 2010;31(2):455–461. doi:10.1002/jcc.21334
45. Motegi A, Masutani M, Yoshioka KI, Bessho T. Aberrations in DNA repair pathways in cancer and therapeutic significances. *Semin Cancer Biol*. 2019;58:29–46. doi:10.1016/j.semcancer.2019.02.005
46. Miranda A, Hamilton PT, Zhang AW, et al. Cancer stemness, intratumoral heterogeneity, and immune response across cancers. *Proc Natl Acad Sci U S A*. 2019;116(18):9020–9029. doi:10.1073/pnas.1818210116
47. Pardoll DM. The blockade of immune checkpoints in cancer immunotherapy. *Nat Rev Cancer*. 2012;12(4):252–264. doi:10.1038/nrc3239
48. Yarchoan M, Hopkins A, Jaffee EM. Tumor mutational burden and response rate to PD-1 inhibition. *N Engl J Med*. 2017;377(25):2500–2501. doi:10.1056/NEJMc1713444
49. Samstein RM, Lee CH, Shoushtari AN, et al. Tumor mutational load predicts survival after immunotherapy across multiple cancer types. *Nat Genet*. 2019;51(2):202–206. doi:10.1038/s41588-018-0312-8
50. Joshi SS, Badgwell BD. Current treatment and recent progress in gastric cancer. *CA Cancer J Clin*. 2021;71(3):264–279. doi:10.3322/caac.21657
51. Chalmers ZR, Connelly CF, Fabrizio D, et al. Analysis of 100,000 human cancer genomes reveals the landscape of tumor mutational burden. *Genome Med*. 2017;9(1):34. doi:10.1186/s13073-017-0424-2
52. Yamamoto H, Watanabe Y, Maehata T, Imai K, Itoh F. Microsatellite instability in cancer: a novel landscape for diagnostic and therapeutic approach. *Arch Toxicol*. 2020;94(10):3349–3357. doi:10.1007/s00204-020-02833-z
53. Goluboff ET. Exisulind, a selective apoptotic antineoplastic drug. *Expert Opin Investig Drugs*. 2001;10(10):1875–1882. doi:10.1517/13543784.10.10.1875
54. Liu L, Li H, Underwood T, et al. Cyclic GMP-dependent protein kinase activation and induction by exisulind and CP461 in colon tumor cells. *J Pharmacol Exp Ther*. 2001;299(2):583–592. doi:10.1016/S0022-3565(24)29266-1
55. Barone I, Giordano C, Bonofiglio D, Andò S, Catalano S. Phosphodiesterase type 5 and cancers: progress and challenges. *Oncotarget*. 2017;8(58):99179–99202. doi:10.18632/oncotarget.21837
56. Rakhshandehroo M, Knoch B, Müller M, Kersten S. Peroxisome proliferator-activated receptor alpha target genes. *PPAR Res*. 2010;2010:1–20. doi:10.1155/2010/612089
57. You M, Gao J, Jin J, Hou Y. PPAR $\alpha$  enhances cancer cell chemotherapy sensitivity by autophagy induction. *J Oncol*. 2018;2018:6458537. doi:10.1155/2018/6458537
58. Maggiora M, Oraldi M, Muzio G, Canuto RA. Involvement of PPAR $\alpha$  and PPAR $\gamma$  in apoptosis and proliferation of human hepatocarcinoma HepG2 cells. *Cell Biochem Funct*. 2010;28(7):571–577. doi:10.1002/cbf.1691
59. Xue J, Zhu W, Song J, et al. Activation of PPAR $\alpha$  by clofibrate sensitizes pancreatic cancer cells to radiation through the Wnt/ $\beta$ -catenin pathway. *Oncogene*. 2018;37(7):953–962. doi:10.1038/ncr.2017.401
60. Chandran K, Goswami S, Sharma-Walia N. Implications of a peroxisome proliferator-activated receptor alpha (PPAR $\alpha$ ) ligand clofibrate in breast cancer. *Oncotarget*. 2016;7(13):15577–15599. doi:10.18632/oncotarget.6402

Journal of Inflammation Research

Publish your work in this journal

The Journal of Inflammation Research is an international, peer-reviewed open-access journal that welcomes laboratory and clinical findings on the molecular basis, cell biology and pharmacology of inflammation including original research, reviews, symposium reports, hypothesis formation and commentaries on: acute/chronic inflammation; mediators of inflammation; cellular processes; molecular mechanisms; pharmacology and novel anti-inflammatory drugs; clinical conditions involving inflammation. The manuscript management system is completely online and includes a very quick and fair peer-review system. Visit <http://www.dovepress.com/testimonials.php> to read real quotes from published authors.

Submit your manuscript here: <https://www.dovepress.com/journal-of-inflammation-research-journal>

Dovepress  
Taylor & Francis Group